

Symmetries and Spectrum of SU(2) Lattice Gauge Theory at Finite Chemical Potential

Simon Hands^a, John B. Kogut^b, Maria-Paola Lombardo^c, Susan E. Morrison^a

^a *Department of Physics, University of Wales Swansea,
Singleton Park, Swansea, SA2 8PP, U.K.*

^b *Department of Physics, University of Illinois at Urbana-Champaign
1110 West Green Street, Urbana, IL 61801-3080, U.S.A.*

^c *Istituto Nazionale di Fisica Nucleare, Laboratori Nazionali del Gran Sasso,
I-67010 Assergi (AQ), Italy **

and

Fakultät für Physik, Universität Bielefeld, Postfach 100 31, D-33501 Bielefeld, Germany

Abstract

We study SU(2) Lattice Gauge Theory with dynamical fermions at non-zero chemical potential μ . The symmetries special to SU(2) for staggered fermions on the lattice are discussed explicitly and their relevance to spectroscopy and condensates at non-zero chemical potential are considered. Using the molecular dynamics algorithm on small lattices we find qualitative changes in the theory's spectroscopy at small and large values of μ . This preliminary study should lay the groundwork for future large scale simulations.

I. INTRODUCTION

Simulations of gauge theories with dynamical fermions using the SU(2) colour group at nonzero density where the action is still real can be performed using standard algorithms, such as hybrid molecular dynamics [1] or hybrid Monte Carlo [2]. These algorithms fail dramatically for QCD which has a complex action once the quark chemical potential $\mu \neq 0$ [3]. Attempts to simulate field theories with complex actions, such as QCD with a nonzero chemical potential, include 1. Langevin algorithms, 2. the Glasgow algorithm pioneered by I. Barbour [4], and 3. analytic extensions of simulations at imaginary chemical potential. None of these methods has succeeded. The complex Langevin algorithms suffer from uncontrollable instabilities, the Glasgow algorithm requires statistics that grow at least as fast as the exponential of the size of the system, and simulations at imaginary chemical potential provide no discernable hints of transitions at real values of μ . These failures are particularly painful because, unlike other phenomena which are not qualitatively sensitive to the gauge

*Current address

group, the physics of field theories at $\mu \neq 0$ is crucially dependent on the gauge group. These points will be made clear below where SU(2) will be considered in detail. Very briefly, baryons and mesons are essentially identical in the SU(2) theory, so all the special features of QCD at nonzero chemical potential which depend on qualitatively different meson and baryon spectroscopy are lost. Of even more significance to the scenarios to be discussed below is the fact that diquarks in the SU(2) theory can be gauge singlets while they cannot be singlets in SU(3). So, if we search for and find strong diquark correlations and/or condensates in the SU(2) theory, these results may have no bearing on such phenomena in the SU(3) theory. The energetics of condensate formation in SU(3) is more challenging, both conceptually and computationally, than in SU(2).

All of these points have conspired to lead researchers, both using lattice methods or crude analytic methods such as instanton models or mean field approaches based on gap equations of simplified field theories, to reconsider SU(2). This will be done below, based on the hope that a controlled and detailed understanding of the SU(2) theory at $\mu \neq 0$ will give some insight into a subset of the phenomena expected in QCD. A quantitative study of QCD at nonzero μ must await further breakthroughs.

The simplest scenario for QCD with $\mu \neq 0$, which we shall refer to as the *standard scenario*, predicts that as μ is increased, observables such as the chiral condensate $\langle \bar{q}q \rangle$, which is non-zero in the vacuum, and quark number density n remain constant until $\mu_o \sim m_{lb}/N_c$, where m_{lb} denotes the mass of the lightest baryon in the spectrum, whereupon a non-zero density of quarks is induced into the ground state, corresponding to a state of nuclear (or hadronic) matter. At some $\mu_c \geq \mu_o$ chiral symmetry should be restored in a (*first order*) transition, resulting in a state of quark matter. Above μ_c there are competing effects governing the quarks' influence on the gluon degrees of freedom. On the one hand, we expect enhanced screening due to quasi-massless virtual $q\bar{q}$ pairs as the chiral symmetries are restored; on the other, we expect the contribution to screening from $q\bar{q}$ pairs lying deep within the Fermi surface to be suppressed for kinematic reasons.

In Figure 1 we present a tentative phase diagram for the standard scenario at zero temperature in SU(2) in the (m, μ) plane. The dotted line corresponds to $\mu_o(m)$, separating a vacuum phase in which $n \equiv 0$ from a phase of “nuclear matter” with $n > 0$. The curvature of this line reflects the expected behaviour $m_{lb} \propto \sqrt{m}$ (note that the lightest baryon in SU(2) gauge theory is degenerate with the pion, and hence becomes massless in the chiral limit by standard PCAC arguments). The solid line corresponds to $\mu_c(m)$, which again is expected to scale as \sqrt{m} : since the chiral condensate $\langle \bar{q}q \rangle$ is never vanishing for $m > 0$, it is not clear *a priori* whether this line demarcates a genuine phase separation, or whether there may in principle be an end-point; this uncertainty is reflected by the question mark (the issue of whether there is a phase separation between “confined” and “deconfined” phases is problematic with dynamical fermions). Note that in the chiral limit both critical values of the chemical potential tend to zero.

Further motivation for investigation of the model comes from recent speculation that the ground state of dense baryonic matter may be more exotic [5] [6]. On the assumption that at high density and zero temperature the quarks have a large Fermi surface, then it is natural to suppose that Bose condensation of quark pairs in the vicinity of the surface takes place, leading to the breaking of the global symmetry of baryon number, and hence superfluidity, and/or even the local gauge symmetry, leading to “color superconductivity”.

This phenomenon would be signalled by a non-vanishing *diquark condensate* $\langle qq \rangle$. As pointed out above, for $N_c = 2$ the situation is qualitatively simpler than what might happen in $SU(3)$: since a $SU(2)$ diquark condensate does not break gauge invariance, its formation would not lead to color superconductivity.

The first lattice analysis of two colors QCD with non-vanishing chemical potential which pointed out the relevance of diquark condensates was a quenched simulation [7] performed in the strong coupling limit $g^2 = \infty$; the results were then compared with analytical predictions obtained from a $1/d$ expansion combined with a mean field analysis, and further confirmed by (nearly exact) monomer-dimer simulations [8]. For the $SU(2)$ theory at $g^2 = \infty$, $T = 0$, $\mu \neq 0$ it was concluded that there is **no chiral symmetry restoring transition**. The simulations suggested that the chiral condensate $\langle \bar{q}q \rangle$ actually vanishes for all $\mu \neq 0$ in the limit $m \rightarrow 0$, while $\langle qq \rangle \neq 0$ for $\mu > m_\pi/2$, thus spontaneously breaking both the $U(1)_V$ global symmetry associated with conservation of baryon number and the chiral symmetry. The simulation results were explained by noticing that the chiral condensate rotates to a baryonic diquark condensate. A baryonic source term was introduced in a mean field analysis and in the dimer calculations but not in exact (hybrid) simulations. The spontaneous breakdown of the $U(1)_V$ symmetry is believed to be a direct consequence of the introduction of a chemical potential. A quenched study of the chiral condensate for two-colors QCD has been published [9].

A detailed analytic study [10] confirms that in the instanton vacuum, at $T=0$, $\mu > m_\pi/2$ the stable phase of the two colour model is indeed a phase with diquark condensation, in agreement with the early lattice studies and the more qualitative discussions reviewed above.

In section II we shall give a detailed outline of the global symmetries of staggered lattice fermions in the fundamental representation of $SU(2)$, and show that the gauge interaction between quark pairs is identical to that between quark and anti-quark. In the chiral and zero-density limits a rotation between ground states with $\langle \bar{q}q \rangle \neq 0$ and $\langle qq \rangle \neq 0$ can thus be performed at zero energy cost, and the two condensates are physically indistinguishable. For $m \neq 0$, $\mu \neq 0$, the analysis must be refined; now the diquark condensate acts as an order parameter signalling the spontaneous breakdown of baryon number conservation. On the assumption that a diquark condensate forms at sufficiently high density we find it plausible that a genuine phase separation occurs, between a normal low density phase with $\langle qq \rangle = 0$ and a high density superfluid phase with $\langle qq \rangle \neq 0$ (as we shall see below, the $\langle qq \rangle$ condensate which seems most likely to form is gauge invariant, and does not give rise to superconductivity in this case). This is shown as a solid line in the tentative phase diagram of Figure 2; the curvature of the line this time reflects the fact that at large Fermi energies asymptotic freedom should weaken the interaction between quark pairs and thus favour the chiral condensate as m is increased. Once again the onset for thermodynamics is expected to occur for $\mu_o \propto m_\pi$, and this is shown by the dotted line.

By further increasing $\mu > \mu_o \simeq m_\pi/2$ diquarks could begin to populate the vacuum producing the ordinary cold nuclear matter phase of $SU(2)$ gauge theory. If the dynamics favor pairing, they could condense. Of course, this phenomenon would have to compete with the free quark phase. Computer simulations which are sensitive to relatively small energy differences could, in principle, find the separation between $\mu_o \simeq m_\pi/2$ and μ_c and assess the physical phase between the solid and dotted line in the phase diagram outlined in Figure 2.

In this paper we present an analysis of the symmetries of the staggered lattice fermion

action. We identify Goldstone modes appropriate to the staggered fermion lattice action in the regimes of low and high baryon density, which enables a tentative classification of the spectrum of light excitations in each regime. We then present numerical results for unquenched simulations of two colours QCD at $\beta = 1.3$ on small lattices, which suggests that for $N_c = 2$ the rotation of the chiral condensate into a diquark condensate observed at infinite coupling is likely to occur also at this coupling, and we establish the level ordering in the particle spectrum in the high energy phase.

II. ACTION AND SYMMETRIES

We will outline plausible patterns of symmetry breaking for SU(2) lattice gauge theory with fermions in the fundamental representation of the gauge group. We emphasize the distinction between the model with continuum fermions in a pseudoreal representation (such as the **2** of SU(2)) which has the symmetry breaking pattern $SU(2N_f) \rightarrow Sp(2N_f)$ in contrast to the lattice model with staggered fermions which, as we shall outline below, has the unorthodox pattern $SU(2N_f) \rightarrow O(2N_f)$. We also consider the consequences of introducing a chemical potential corresponding to non-zero baryon density.

Let us start with the kinetic term in the lattice action for a gauged isospinor doublet (**2**) of staggered fermions $\chi, \bar{\chi}$. For clarity we will consider $N = 1$ flavors, although this will be generalised when the numerical simulations are discussed.

$$S_{kin} = \sum_{x, \nu=1,3} \frac{\eta_\nu(x)}{2} [\bar{\chi}(x) U_\nu(x) \chi(x + \hat{\nu}) - \bar{\chi}(x) U_\nu^\dagger(x - \hat{\nu}) \chi(x - \hat{\nu})] \\ + \sum_x \frac{\eta_t(x)}{2} [\bar{\chi}(x) e^\mu U_t(x) \chi(x + \hat{t}) - \bar{\chi}(x) e^{-\mu} U_t^\dagger(x - \hat{t}) \chi(x - \hat{t})] \quad (2.1)$$

The U 's are 2×2 complex matrices acting on color indices. The chemical potential enters via the timelike links in the standard way. It is straightforward to rearrange (2.1), using the Grassmann nature of $\chi, \bar{\chi}$, the fact that $\eta_\mu(x) \equiv (-1)^{x_0 + \dots + x_{\mu-1}} = \eta_\mu(x \pm \hat{\mu})$, and the property $\tau_2 U_\mu \tau_2 = U_\mu^*$, where τ_2 is a Pauli matrix:

$$S_{kin} = \sum_{x \text{ even}, \nu=1,3} \frac{\eta_\nu(x)}{2} [\bar{X}_e(x) U_\nu(x) X_o(x + \hat{\nu}) - \bar{X}_e(x) U_\nu^\dagger(x - \hat{\nu}) X_o(x - \hat{\nu})] \\ + \sum_{x \text{ even}} \frac{\eta_t(x)}{2} \left[\bar{X}_e(x) \begin{pmatrix} e^\mu & 0 \\ 0 & e^{-\mu} \end{pmatrix} U_t(x) X_o(x + \hat{t}) - \bar{X}_e(x) \begin{pmatrix} e^{-\mu} & 0 \\ 0 & e^\mu \end{pmatrix} U_t^\dagger(x - \hat{t}) X_o(x - \hat{t}) \right] \quad (2.2)$$

with the definitions

$$\bar{X}_e = (\bar{\chi}_e, -\chi_e^{tr} \tau_2) \quad : \quad X_o = \begin{pmatrix} \chi_o \\ -\tau_2 \bar{\chi}_o^{tr} \end{pmatrix}. \quad (2.3)$$

The sum in (2.2) is only over even sites, ie. those defined by $\varepsilon(x) = (-1)^{x_1 + x_2 + x_3 + x_4} = +1$, and the subscripts emphasise that the \bar{X} fields are only defined on even sites, and the X on odd.

Now, in the original action (2.1) there are two manifest global U(1) symmetries:

$$\chi \mapsto e^{i\alpha} \chi \quad \bar{\chi} \mapsto \bar{\chi} e^{-i\alpha} \quad : \quad \chi \mapsto e^{i\alpha\varepsilon} \chi \quad \bar{\chi} \mapsto \bar{\chi} e^{i\alpha\varepsilon}, \quad (2.4)$$

the first (U(1)_V) corresponding to conservation of baryon number and the second, which holds only in the chiral limit $m = 0$ and which we will call U(1)_A, corresponds to a form of axial charge conservation. In (2.2) we can see that in the chiral limit at zero density (ie. for $\mu = m = 0$) both are subsumed in a larger U(2) symmetry (because exact global symmetries are non-anomalous in lattice formulations, the full symmetry is U(2); in a continuum approach the axial anomaly would reduce it to SU(2)):

$$X_o \mapsto V X_o \quad \bar{X}_e \mapsto \bar{X}_e V^\dagger \quad V \in \text{U}(2). \quad (2.5)$$

By introducing a non-zero chemical potential we reduce the U(2) symmetry of the lattice action to U(1)_V \otimes U(1)_A, and by introducing a bare mass we reduce it to U(1)_V. This will be important when we identify and compare the Goldstone modes present in the low and high density phases.

A. Qualitative Discussion of Symmetries and Spectrum

1. $\mu = 0.0$

As anticipated in the Introduction, when $\mu = 0$ quarks and antiquarks belong to equivalent representations: there is a symmetry transformation which turns a chiral condensate into a diquark one. In other words, there is only one discernable condensate, $\langle \bar{q}q \rangle^2 + \langle qq \rangle^2$, whose orientation in the chiral sphere is selected by the explicit breaking term.

Recall that the extra quark-antiquark symmetry enlarges the continuous global symmetry of the lattice Action from $U(f) \times U(f)$ to $U(2f)$, while the subgroup which leaves the mass term $\langle \bar{q}q \rangle^2 + \langle qq \rangle^2$ invariant is O(2f) [11]. By applying a generic O(2f) transformation to the mass term $\bar{\chi}\chi$ we identify the following set of operators which might form condensates:

$$\text{scalar} \quad \chi_1 \bar{\chi}_1 + \chi_2 \bar{\chi}_2 \quad \text{pseudoscalar} \quad \varepsilon(\chi_1 \bar{\chi}_1 + \chi_2 \bar{\chi}_2) \quad (2.6)$$

$$\text{scalar diquark} \quad \chi_1 \chi_2 - \chi_2 \chi_1 \quad \text{pseudoscalar diquark} \quad \varepsilon(\chi_1 \chi_2 - \chi_2 \chi_1) \quad (2.7)$$

$$\text{scalar antiquark} \quad \bar{\chi}_1 \bar{\chi}_2 - \bar{\chi}_2 \bar{\chi}_1 \quad \text{pseudoscalar antiquark} \quad \varepsilon(\bar{\chi}_1 \bar{\chi}_2 - \bar{\chi}_2 \bar{\chi}_1) \quad (2.8)$$

where the lower index labels colour. The first line displays the usual pseudoscalar and scalar condensates. The second (third) line corresponds to diquark (antiquark) condensates, scalar and pseudoscalar. This simple minded quantum number assignment is done by considering that quark – quark and quark-antiquark pairs have opposite relative parity, and will be confirmed by the rigorous analysis below. See also the interesting discussions in [12].

Consider now quark propagation from a source at 0 to the point x . The propagator G_{ij} (i, j color index) is an SU(2) matrix:

$$G_{ij} = \begin{pmatrix} a & b \\ -b^\star & a^\star \end{pmatrix} \quad (2.9)$$

By taking its correlations in the appropriate sector of quantum numbers we form meson and diquark operators. We shall limit ourselves to the local sector of the spectrum and focus on the zero momentum *connected* propagators of the scalar and pseudoscalar mesons and diquarks. The scalar meson propagator will thus be an isovector, which we will call δ , following QCD notation.

The meson ($q\bar{q}$) and diquark (qq) and antidiquark ($\bar{q}\bar{q}$) propagators at $\mu = 0$ are constructed from G_{ij} as follows:-

$$\text{pion} \quad \text{tr}GG^\dagger = (a^2 + b^2) \quad (2.10)$$

$$\text{scalar meson} \quad \varepsilon \text{tr}GG^\dagger = \varepsilon(a^2 + b^2) \quad (2.11)$$

$$\text{scalar } qq \quad \det G = (a^2 + b^2) \quad (2.12)$$

$$\text{scalar } \bar{q}\bar{q} \quad \det G^\dagger = (a^2 + b^2) \quad (2.13)$$

$$\text{pseudoscalar } qq \quad \varepsilon \det G = \varepsilon(a^2 + b^2) \quad (2.14)$$

$$\text{pseudoscalar } \bar{q}\bar{q} \quad \varepsilon \det G^\dagger = \varepsilon(a^2 + b^2) \quad (2.15)$$

The notable feature of the propagators at $\mu = 0$ is the exact degeneracies of the pion, scalar qq and scalar $\bar{q}\bar{q}$ and of the scalar meson, pseudoscalar qq and pseudoscalar $\bar{q}\bar{q}$. This can also be understood as being due to quarks and anti-quarks having opposite intrinsic parities, whereas the qq and $\bar{q}\bar{q}$ interactions due to gluon exchange are identical. We then identify two orthogonal directions in the chiral space:

- a) π - scalar diquark - scalar antidiquark
- b) δ - pseudoscalar diquark - pseudoscalar antidiquark

2. $\mu \neq 0$

When $\mu \neq 0$ the symmetry is reduced to that of staggered fermions, i.e. $U_A(1) \times U_V(1)$ [8], however the possibility of diquark condensation¹ could lead to unusual patterns of chiral symmetry.

The condensate will tend to rotate in chiral space as μ increases, rotating into a purely diquark direction for large μ . However, as μ increases and the symmetry in chiral space is reduced, as will be discussed below, the rotation will no longer be “trivial” (as it would be at zero chemical potential) and the new vacuum would be physically distinct from the original one. See also the interesting comments in [10].

Consider the Dirac kinetic operator \mathcal{D} for staggered fermions. At $\mu = 0$ the relation $\mathcal{D}^\dagger = -\mathcal{D}$ holds. For $\mu \neq 0$ the fact that e^μ ($e^{-\mu}$) multiplies the forward (backward) timelike gauge links in the lattice action means that $\mathcal{D}^\dagger \neq -\mathcal{D}$, because in the matrix \mathcal{D}^\dagger , $e^{-\mu}$ (e^μ) now multiplies the forward (backward) links. Consequently the propagators G and G^\dagger are no longer trivially related as they are at $\mu = 0$. The composite propagators can be computed as follows [14]:

$$\begin{array}{ll} \text{pion} & \text{tr}G(\mu)G^\dagger(-\mu) \\ \text{scalar } qq & \det G(\mu) \end{array} \quad (2.16)$$

¹ The conditions leading to the Vafa Witten theorem do not hold here.

with analogous formulas for the scalar meson and pseudoscalar qq .

Note for $\mu \neq 0$, that although the diquark Goldstone modes in (2.24) contain both $\chi\chi$ and $\bar{\chi}\bar{\chi}$ operators, we expect the physical states in the high density ground state to be formed predominantly of quarks rather than anti-quarks. We see from (2.16) that for $\mu \neq 0$ the pion is no longer degenerate with the scalar qq ; correspondingly the degeneracy of the scalar meson with the pseudoscalar qq is also broken.

Finally, consider the ‘‘baryonic’’ pion [13] which is believed to be responsible for the failure of quenched 3 colours QCD (or indeed for any treatment with a real path integral measure proportional to $\det M^\dagger M$). The propagator would be:

$$\text{baryonic pion} \quad \text{tr} G(\mu) G^\dagger(\mu) \quad (2.17)$$

We see that for the 2 colours theory a consequence of the fact that the quark propagators are SU(2) matrices even for $\mu \neq 0$ is that the baryonic pion is degenerate with the scalar diquark via eqns. (2.10,2.12): in SU(2) at nonzero chemical potential it is still possible to express a diquark propagator as a positive definite quantity.

B. Rigorous discussion of symmetries and spectrum

At zero density ($\mu = 0$), we expect the model to display spontaneous chiral symmetry breaking, with a chiral condensate of the same form as the mass term $m \sum_x \bar{\chi}(x) \chi(x)$. In terms of the X, \bar{X} fields, introduced in (2.3),

$$\bar{\chi}\chi = \frac{1}{2} \left[\bar{X}_e \begin{pmatrix} & 1 \\ 1 & \end{pmatrix} \tau_2 \bar{X}_e^{tr} + X_o^{tr} \begin{pmatrix} & 1 \\ 1 & \end{pmatrix} \tau_2 X_o \right]. \quad (2.18)$$

Of course, the condensate breaks the global symmetry (2.5): the residual symmetry is generated by the subgroup which leaves invariant the symmetric form $\begin{pmatrix} 0 & 1 \\ 1 & 0 \end{pmatrix}$, whose most general element is $\begin{pmatrix} e^{i\alpha} & \\ & e^{-i\alpha} \end{pmatrix}$, which generates $U(1)_V$. We thus identify the pattern of chiral symmetry breaking as $U(2) \rightarrow U(1)$ for $\mu = 0$.

For $\mu = 0$ the number of broken generators is 3 (since $\dim U(2)=4$), so we expect the spectrum of the model to contain three massless Goldstone modes. These can be found by considering infinitesimal rotations of the condensate (2.18) by $V_\delta = \mathbb{1} + i\delta\lambda$, with λ one of the $U(2)$ generators $\{\mathbb{1}, \tau_i\}$, and identifying the mode as the coefficient of $O(\delta)$. The results are

$$\begin{aligned} \mathbb{1} &\Rightarrow \bar{\chi}\varepsilon\chi \\ \tau_1 &\Rightarrow \chi^{tr} \tau_2 \chi - \bar{\chi} \tau_2 \bar{\chi}^{tr} \\ \tau_2 &\Rightarrow \chi^{tr} \tau_2 \chi + \bar{\chi} \tau_2 \bar{\chi}^{tr} \\ \tau_3 &\Rightarrow \mathbb{1} \end{aligned} \quad (2.19)$$

As expected, the first of these modes is the familiar pion $\bar{\chi}\varepsilon\chi$, which is a pseudoscalar since it is odd under the lattice definition of parity:

$$x = (x_0, x_1, x_2, x_3) \mapsto x' = (x_0, 1 - x_1, 1 - x_2, 1 - x_3) \\ \chi(x) \mapsto (-1)^{x'_1+x'_3} \chi(x'), \quad ; \quad \bar{\chi}(x) \mapsto (-1)^{x'_1+x'_3} \bar{\chi}(x'). \quad (2.20)$$

The second two, however, are gauge invariant linear combinations of scalar diquark $\chi\chi$ and $\bar{\chi}\bar{\chi}$ states. The $\mathbb{1}$ indicates that rotations generated by τ_3 leave the condensate invariant. These states carry baryon number and although they would be true Goldstone modes only in the chiral limit and at $\mu = 0$, by continuity we expect them to be light states in the low density regime with masses vanishing as \sqrt{m} . For $\mu \neq 0$ of the three states identified only the pion remains a Goldstone mode. The pion is generated by $\mathbb{1}$ and is associated with spontaneous breaking of $U(1)_A$. The $U(1)_V$ rotation generated by τ_3 , as discussed above, leaves the condensate invariant.

The symmetry breaking described here is notable because it is distinct from the $SU(2N_f) \rightarrow Sp(2N_f)$ predicted for continuum fermions in a pseudoreal gauge representation such as the **2** of $SU(2)$ [15]. This discrepancy between lattice and continuum has been known for some time [11] [16]. For a complete classifications of the possible patterns of chiral symmetry breaking see [17]. For patterns of chiral symmetry breaking the roles of fundamental and adjoint representations appear to be reversed on the lattice [18].

At high density ($\mu \gg m_\pi/2$), let us postulate that a large Fermi surface will promote the formation of a diquark condensate. Which condensate forms is a dynamical question, since in principle many diquark wavefunctions can be written down. It is instructive to consider a “maximally attractive channel” (MAC) for the formation of the condensate. We proceed by making the following assumptions about the MAC condensate:

- (a) The condensate is gauge invariant.
- (b) The condensate is invariant under lattice parity (2.20) and exhibits no preferred spatial orientation.
- (c) The MAC condensate is as local as possible in the $\chi, \bar{\chi}$ fields.
- (d) The condensate wavefunction is anti-symmetric under exchange of fields.

Of these four assumptions, only (d) should be considered inviolate [5] [6]. For isospinor fermions, however, it is straightforward to write down a local condensate qq_2 which satisfies (a) – (d):

$$qq_2 = \frac{1}{2} \left[\chi^{tr}(x) \tau_2 \chi(x) + \bar{\chi}(x) \tau_2 \bar{\chi}^{tr}(x) \right]. \quad (2.21)$$

The relative + sign between the two terms is not arbitrary; this can be seen by considering a two-point function $\langle \chi\chi(x) \bar{\chi}\bar{\chi}(y) \rangle$, which in a vacuum with a diquark condensate will cluster at large separations into $\langle \chi\chi \rangle \langle \bar{\chi}\bar{\chi} \rangle$ [19] [20]. We know that the scalar diquark propagator is proportional to the determinant of an $SU(2)$ matrix (see eqs.(2.12 - 2.15) above), and hence positive definite; therefore the $\chi\chi$ and $\bar{\chi}\bar{\chi}$ condensates must form with the same sign.

In terms of the X, \bar{X} fields the condensate is written

$$qq_2 = \frac{1}{2} \left[\bar{X}_e \begin{pmatrix} 1 & \\ & -1 \end{pmatrix} \tau_2 \bar{X}_e^{tr} + X_o^{tr} \begin{pmatrix} 1 & \\ & -1 \end{pmatrix} \tau_2 X_o \right]. \quad (2.22)$$

The fascinating feature of this $SU(2)$ model is that the diquark condensate (2.22) can be obtained from the chiral condensate (2.18) by an explicit global $U(2)$ rotation:

$$V = \frac{i}{\sqrt{2}} \begin{pmatrix} 1 & 1 \\ -1 & 1 \end{pmatrix}. \quad (2.23)$$

Therefore the pattern of symmetry breaking for $m = \mu = 0$ remains $U(2) \rightarrow U(1)$, but the unbroken symmetry is no longer $U(1)_V$. The chiral condensate is equivalent to the diquark condensate due to the symmetry transformation relating them. There is only one discernable condensate whose orientation in the chiral sphere is selected by the explicit breaking term. In lattice simulations we select the chiral condensate $\langle \bar{q}q \rangle$ because the bare mass $m \neq 0$. In principle by setting the bare mass to zero and including a diquark source term we would obtain a diquark condensate $\langle qq \rangle$ at $\mu = 0$.

For non-zero density one might naively expect that as μ increases with respect to m the condensate gradually *rotates* from a chiral $\langle \bar{q}q \rangle$ to a diquark $\langle qq \rangle$. Actually the true behaviour is more subtle, because once $m \neq 0$, $\mu \neq 0$ the rotation is no longer trivial; the vacuum at large μ must be distinct from that at $\mu = 0$. This fact is reflected by different numbers of Goldstone modes in high and low density regimes; we shall argue that there is a phase separation between low and high density, with the diquark condensate acting as order parameter.

We can check this by analysing the Goldstone modes obtained by $U(2)$ rotations of the diquark condensate (2.22):

$$\begin{aligned} \mathbb{1} &\Rightarrow \chi^{tr} \tau_2 \varepsilon \chi + \bar{\chi} \tau_2 \varepsilon \bar{\chi}^{tr} \\ \tau_1 &\Rightarrow \mathbb{1} \\ \tau_2 &\Rightarrow \bar{\chi} \chi \\ \tau_3 &\Rightarrow \chi^{tr} \tau_2 \chi - \bar{\chi} \tau_2 \bar{\chi}^{tr} \end{aligned} \quad (2.24)$$

Just as before, in the chiral limit for $\mu = 0$, there are three Goldstone modes, a scalar $q\bar{q}$ state, a scalar qq state (which is orthogonal to the condensate), and a pseudoscalar qq state. The spectrum of massless states has identical quantum numbers to those of (2.19) in this limit. The pseudoscalar $q\bar{q}$, i.e. the pion, is *no longer* a Goldstone particle in the high density vacuum. For $\mu \neq 0$ we retain two of these Goldstone modes: firstly the pseudoscalar diquark generated by $\mathbb{1}$ and associated with spontaneous breaking of $U(1)_A$ which is a pseudo-Goldstone for $m \neq 0$; secondly the scalar diquark generated by τ_3 and associated with spontaneous breaking of $U(1)_V$. This second state remains an exact Goldstone mode even once $m \neq 0$, since there are no terms in (2.1) which explicitly break this symmetry. Therefore we expect a level ordering (light \rightarrow heavy) in the high density regime of scalar diquark (massless), pseudoscalar diquark, scalar meson, pion. We will see below in sections IV and V to what extent these predictions are borne out in the simulations.

Recall that away from the chiral limit, in the low density regime but for $\mu \neq 0$ we have no exact Goldstones, but only three light states, the pion and two scalar diquarks. The fact that the low and high density regimes are characterised by different numbers of massless modes indicates that they should be separated by a true phase transition at some $\mu = \mu_c$. This is indicated in the proposed phase diagram of figure 2. The Goldstone count in the diagram is as follows: zero in the region to the right of the solid line; one in the region to

the left of this line where $\langle qq \rangle \neq 0$; two in the chiral limit along the μ -axis; finally three at the U(2) symmetric point at the origin.

Finally, we should discuss the effects of using the hybrid molecular dynamics [1] (or hybrid Monte Carlo [2]) algorithm to simulate the model. The functional integral measure contains a factor $\det^N M^\dagger M$, with M the fermion matrix for one flavor of staggered fermion. Since $\det M^\dagger = \det M^* = \det \tau_2 M \tau_2 = \det M$, then we know the simulation describes $2N$ identical flavors of staggered fermion. It can be shown that $\det M$ is positive definite for $\mu \neq 0$ [21] therefore one could in principle “take the square root” by setting $N = \frac{1}{2}$ in a hybrid algorithm. To reduce the number of flavors in a simulation at zero chemical potential using staggered fermions, standard practice is to use even-odd partitioning. This relies on the equality of the fermion determinant on the even sublattice with that on the odd sublattice which means that we require $\det M^\dagger = \det M$, a relation which no longer holds for $\mu \neq 0$. Thus we are constrained to a minimum of $N_f = 8$ continuum flavours in our simulation (recall that the number of physical flavors $N_f = 4N$ for staggered lattice fermions). This should still result in an asymptotically-free theory, since $N_f < \frac{11}{2}N_c$; however, the two-loop coefficient of the beta-function is now positive since $N_f > 34N_c^3/(13N_c^2 - 3)$, which means that the model should exhibit non-trivial fixed-point behaviour in the far infra-red [22]. The question of confinement/deconfinement is thus further complicated. A recent non-perturbative calculation by Appelquist and Sannino [23] suggests indeed that the onset of the conformal phase is at $N_f > 3.9N_c$. That would place our 8 flavours 2 colours results in the conformal phase; however, on the lattice volumes considered here we have seen no indication of an ‘exotic’ behaviour.

The symmetries of the lattice model for $N = 2$ flavours of staggered fermion will be very similar to the $N = 1$ case discussed above because (i) the mass term and hence the chiral condensate will be flavor symmetric, and (ii) the diquark channel we have analysed on the assumption that it is MAC must also be flavor symmetric due to the Pauli exclusion principle. Therefore the whole analysis should go through virtually unchanged, with the resulting pattern of symmetry breaking for $\mu = 0$ of $U(4) \rightarrow O(4)$, with 10 associated Goldstone modes. Of course, all our measurement algorithms to date work in the single flavor sector, therefore we should only “observe” three Goldstone modes. So the special features of the SU(2) gauge theory arise from the fact that the quarks and the anti-quarks belong to equivalent representations which enlarges the continuous global symmetry of the lattice action describing N flavors of staggered fermion from $U(N) \times U(N)$ to $U(2N)$. The subgroup which leaves the mass term invariant is $O(2N)$. In general there are $4N^2 - N(2N - 1) = 2N^2 + N$ broken generators associated with N^2 Goldstone mesons, and $N^2 + N = 2N(N+1)/2$ Goldstone baryons and antibaryons. It is instructive to consider what will happen as the flavor symmetries enlarge in the continuum limit, when we expect the model to describe $N_f = 4N$ quarks. It is currently unclear whether the lattice model in this limit will persist in the non-standard $SU(2N_f) \rightarrow O(2N_f)$ (note the axial anomaly should reemerge in this limit), or assume the orthodox continuum pattern $SU(2N_f) \rightarrow Sp(2N_f)$ [15].

III. SIMULATIONS

In this initial study of two colours QCD at non-zero chemical potential we used a standard hybrid molecular dynamics algorithm [1,24]. Since we cannot use even-odd partitioning when

$\mu \neq 0$ we were constrained to the minimal value of 8 continuum flavours.

We simulated at $\mu \neq 0$ at couplings: $\beta = 1.3$ where the system was in the phase of broken chiral symmetry at $\mu = 0$. Most of the simulations were on 6^4 lattices however we studied the mass spectrum on a $6^3 \times 12$ lattice at $\beta = 1.3$ with $m = 0.07$ for $\mu = 0.0, 0.2, 0.4$. Note that although the fermion determinant of the SU(2) theory is positive definite for $\mu \neq 0$, it is likely that value of the fermion determinant has large fluctuations in magnitude when the chemical potential is switched on. In support of this conjecture we found that the simulations numerically intensive for $\mu > m_\pi/2$.

For chemical potential smaller than $m_\pi/2$ simulations were not problematic and in this case we chose $dt = .02$ and ran for 5000 sweeps, after discarding 1000 sweeps for thermalization.

For $\mu \geq m_\pi/2$, we observed several instabilities. Typically, the system was crashed after a few tens of iterations. To combat this we refreshed the system frequently (every 5 sweeps for the gauge fields and 3 for the fermions). In this way we could run for thousands of iterations with $dt = .02$. With the exception of $\mu = .8$, $dt = .05$ worked also. As final strategy, we thermalized with $dt=.05$ for 500 iterations, subsequently reduced dt to $.02$, reequilibrated for 300 sweeps proceeded to measure for 5000 sweeps.

To monitor any possible bias introduced by the frequent refreshment we also continued our runs at $\mu = .6$ with a pure molecular dynamics evolution, which revealed no problem for a few thousands steps (therefore we stopped it).

Clearly, we cannot exclude ergodicity problems.

In Figs. 3 we show the chiral condensate as a function of bare mass m for a range of values of chemical potential. The system is clearly in the broken phase at $\mu = 0.0$ and the chiral condensate decreases quite sharply as μ is increased.

In the standard scenario, we expect that as μ is increased beyond $m_\pi/2$ the ground state populated by quarks will be favoured over the vacuum state; therefore chiral symmetry may be restored for $\mu \geq m_\pi/2$. We found that at $\beta = 1.5$ for $m = 0.1$, the pion mass $m_\pi \simeq 0.8$ while at $\beta = 1.3$ with $m = 0.07$ we find $m_\pi \simeq 0.6$

Behaviour consistent with the standard scenario is reflected in the Figs. 4 where the chiral condensate is plotted as a function of m . At $\beta = 1.3$ and at $\mu = 0.2$ there is a strong m -dependence in the value of the chiral condensate. The chiral transition seems significantly sharper at $m = 0.07$ than it is at $m = 0.05$ as we would expect. See the spectrum section V for a discussion of these results.

IV. PARTICLE SUSCEPTIBILITIES

Measurement of the meson and diquark susceptibilities will allow us to assess the effects of chiral symmetry restoration and, to some extent, explore the level ordering in the particle spectrum [25] which should reflect properties noted in the earlier discussion of symmetries where we identified Goldstone modes in high and low density phases.

In terms of the timeslice propagator $P(t) = \sum_{\mathbf{x}} G'(\mathbf{x}, t)$, the susceptibility, χ , is defined by

$$\chi = \sum_t P(t). \quad (4.1)$$

On the assumption that a particular channel is dominated by a single pole, then χ can be written Z/M_{bs}^2 , where M_{bs} is a bound state mass and Z is a wavefunction renormalisation constant. If we make a second assumption that the Z 's are relatively insensitive to the quantum number of the state, then susceptibility measurements yield information about level ordering without the need for any propagator fitting, and may be a more reliable guide on the small lattice volumes presented here (see however the comments below).

We have measured susceptibilities of the scalar mesons and diquarks, taking into account contributions from connected diagrams only, and plotted the quantity $m\chi$ which we expect (from the Ward identity) to be equal to the chiral condensate in the case of the pion susceptibility. Although the realization of PCAC in this model has yet to be worked out in detail, it is reasonable to assume that in each channel the susceptibility gives a direct measure of the associated condensate.

The degeneracies of the meson and diquark sectors are broken for any $\mu \neq 0$. The pion which is a pseudo-Goldstone for $\mu < m_\pi/2$, becomes heavy in the dense phase whereas the pseudoscalar qq state which is heavy in the low density phase, becomes light in the high density phase. Recall from section II that we expected the scalar diquark to be an exactly massless mode in the high density phase. Unfortunately it is impossible to infer the level ordering directly from the susceptibilities, since the possible occurrence of a plateau prevents it (see the discussion in Sec. V).

The level ordering we infer (lightest to heaviest) from Fig. 5 for the susceptibilities is scalar diquark, pseudoscalar diquark, and a degenerate pion and delta susceptibilities.

Degeneracy of the pion and δ is usually interpreted as a signal for the restoration of $U_A(1)$ symmetry. It would be natural to infer from that a complete suppression of the topological fluctuations induced by the ordering effects of the chemical potential [26].

Rigorous arguments predict that, indeed, the scalar diquark propagator should always be the larger one [27]. However, it is not possible to infer from this a mass level ordering since the scalar propagator has a disconnected component, and because of the multiplicative renormalization of the wavefunction. For these reasons we have performed a mass spectrum calculation which will show that the particle content of the scalar and pseudoscalar diquark propagators is indeed the same and we postpone a detailed comparison of the numerical and analytic results to the spectrum section.

V. PARTICLE SPECTRUM

To extend and verify the information obtained from the susceptibilities we have performed particle spectrum measurements on a lattice with extended temporal direction. We simulated at $\beta = 1.3$, $m = 0.07$ on a $6^3 \times 12$ lattice. The qualitative trends revealed in the susceptibility measurements are the fact that we have a light pion and scalar diquark in the low density phase and two light diquark states in the high density phase. We expect the pion to become heavy and degenerate with the connected contribution to the scalar meson (called δ) for $\mu > m_\pi/2$.

Finite density spectroscopy analysis has been introduced and discussed in [14]. The following symmetries should hold true in the ensemble:

$$G(t) = G(T - t) \quad \text{for mesons} \quad (5.1)$$

$$G(t, \mu) = G(T - t, -\mu) \quad \text{for diquarks} \quad (5.2)$$

The particle propagators for $\mu = 0.0$ and for $\mu = 0.4$ are shown in Fig. 6. At $\mu = 0$ the pion and scalar diquark are degenerate light states while the pseudoscalar diquark and scalar meson are degenerate but comparatively heavy. The propagators are symmetric in time at $\mu = 0$. However at $\mu = 0.4$ the chemical potential induces an asymmetry in the propagators by favouring forwards over backwards propagation. As expected from the susceptibilities, the pion is now a heavy state which is approximately degenerate with the scalar meson. We also note (see Figs. 6 and 7) that at $\mu = 0.4$ $G_{\text{scalar qq}}(t) = G_{\text{pseudoscalar qq}}(t) + p$, where p is a constant. This means that the pole contents of scalar and pseudoscalar diquark propagators are identical, i.e. the scalar and pseudoscalar diquarks are degenerate. We found that p increased as μ was increased, this trend being more clear in the scalar channel where condensation is expected (Fig. 8). If this trend were to persist for a range of lattice volumes then it could be interpreted as evidence for condensation in the scalar diquark channel with $p \propto |\langle qq \rangle|^2$. A similar analysis has been applied to simulations of the 2+1 dimensional Gross-Neveu model [19]; stable plateaux were indeed observed, but the volume scaling of the constant p did not show the expected behaviour. To confirm this scenario one would have to implement an explicit diquark source term jqq and extrapolate the source j to zero: this work is in progress [28].

The dashed lines in Figs. 6 are the results of the fits to

$$G_m(t) = a(e^{-mt} + e^{m(T-t)}) + (-1)^t b(e^{-m_1 t} + e^{m_1(T-t)}) + p \quad (5.3)$$

for the mesons and

$$G_b(t) = ae^{-m_f t} + be^{m_b(T-t)} + p \quad (5.4)$$

for the diquarks.

For the mesons p should be zero and m and m_1 correspond to masses of states with different lattice parity. Since the mesons do not “feel” the effects of the chemical potential the masses of the forward and backward propagating meson states are identical. Although the inclusion of the oscillating term was mandatory for a good fit, very often only the fundamental amplitude and the first mass were meaningfully determined. For $\mu \neq 0$ we expect $m_f \neq m_b$ in the diquark channels, reflecting the different backwards and forward propagations in the dense medium.

The particle masses for the mesons and for the diquark states were measured at $\mu = 0.0, 0.2, 0.4$ and are plotted in Fig. 9. The pion mass increases, while the scalar meson mass decreases as μ is increased and the two particles become approximately degenerate at $\mu \simeq 0.4$ (at zero density $m_\pi/2 \simeq 0.3$). The scalar diquark which is degenerate with the pion at $\mu = 0.0$ is already lighter than the pion at $\mu = 0.2$ and by $\mu = 0.4$ the pseudoscalar and scalar diquarks are apparently considerably lighter than the pion and delta meson.

In conclusion the ordering is as follows: two light (see however the comment below), degenerate diquarks, two heavier, degenerate pion and delta

This ordering is not quite what was predicted in section II, and several comments are in order. First, recall that the predictions of section II are for the σ meson, while the numerical results are for the δ meson. It is certainly possible that the σ is lighter.

Next, the operator (2.12), being manifestly real, may not project onto the true Goldstone mode, which corresponds to fluctuations in the phase of the condensate. It is interesting to note that for diquark condensation, unlike chiral condensation, there is no spacetime quantum number (such as parity) which serves to distinguish transverse (ie. Goldstone) from longitudinal (ie. Higgs) excitations.

A speculative comment is in order. A naive approach to calculating masses in the presence of a chemical potential would suggest that the zero density masses would be shifted downwards by $n \times \mu$, where n is the number of quarks in the state under consideration. This shift merely reflects a change of the reference level of the energy, therefore does not take into account any new dynamics associated with propagation through a dense medium. To appreciate the true dynamical content we plotted, together with the masses themselves, the reference energy $E(\mu) = E(0) - 2\mu$. We do indeed observe that the change of the masses is genuine and not merely a simple shift in the energy scale. However, if we add a shift $n\mu$ to our spectrum results, the data suggest that all the four masses are then nearly degenerate. Note that preliminary calculations in a model field theory suggest precisely this result [27].

Finally, if we estimate the constituent mass from the ρ propagator, as seems reasonable, we would convince ourselves that these states are still bound as $\rho \simeq 1.8 > \pi \simeq 1.2$. In conclusion, the results for the π - δ , and the scalar-pseudoscalar diquarks, masses suggest degenerate, composite, massive, but rather light particles.

VI. SUMMARY AND OUTLOOK

In this study of two colors QCD at non-zero chemical potential with dynamical fermions we have outlined in detail the symmetries of the lattice model and identified the Goldstone modes in the low and high density phases incorporating the possibility of diquark condensation for $\mu > m_\pi/2$. In our preliminary simulations we have established the level ordering of the particle spectrum from the susceptibilities and via direct measurements for several values of μ . The analytic results predict Goldstone states which we have not observed in the simulations. The simulation results indicate four degenerate states at large μ , when the data are referred to the same energy scale, or two couples of degenerate particles if we do not change the energy reference. As discussed in the text, it is conceivable that none of the operators we have implemented are suitable for measuring the Goldstone modes predicted by the analytic calculations. We have noted exact degeneracies at $\mu = 0$ between pion and scalar diquark; scalar meson and pseudoscalar diquark. The pion which is a pseudo-Goldstone in the low density phase becomes heavy in the dense phase whereas the pseudoscalar diquark is heavy in the low density phase but becomes light in the high density phase. For $\mu > m_\pi/2$ the pion and scalar meson δ are approximately degenerate. It would be very interesting to measure the σ which would require the disconnected contributions. It is certainly possible that the sigma and delta masses are different.

It is possible that the rotation of chiral condensate to baryonic condensate first noted in the infinite coupling regime [7] persists in the intermediate and weak coupling regimes and our symmetries analysis supports this. The fact that the scalar and pseudoscalar diquark states are found to be light for $\mu > m_\pi/2$ is also suggestive. In an extension of this work we will implement an explicit diquark source term in a hybrid Monte Carlo simulation and investigate the effects of extrapolating the source to zero [28].

Finally, we notice that while the diquark observables introduced for studying condensation phenomenon display an interesting and peculiar behaviour, there is nothing in the behaviour of the conventional observables discussed here - - chiral condensate, meson spectrum - which requires going beyond the standard scenario. The thermodynamics of this model is considered in a companion paper [29].

ACKNOWLEDGEMENTS

MPL, SEM and SJH received support from EU TMR contract no. ERBFMRXCT97-0122. SEM thanks the Zentrum für Interdisziplinäre Forschung der Universität Bielefeld for hospitality during the early stages of this project. JBK thanks the National Science Foundation (NSF-PHY96-05199) for partial support.

REFERENCES

- [1] S. Duane and J.B. Kogut, Nucl. Phys. **B275** (1986) 398.
- [2] S. Duane, A.D. Kennedy, B.J. Pendleton and D. Roweth, Phys. Lett. **B195** (1987) 216.
- [3] See e.g. Proceedings of *QCD at Finite Baryon Density*, Bielefeld, April 1998, F. Karsch and M.-P. Lombardo, eds, Nucl. Phys. **A 642**, 1998.
- [4] I.M. Barbour and A.J. Bell, Nucl. Phys. **B372** (1992) 385.
- [5] M. Alford, K. Rajagopal and F. Wilczek, Phys. Lett. **B422** (1998) 247; Nucl. Phys. **B537** (1999) 443.
- [6] R. Rapp, T. Schäfer, E.V. Shuryak and M. Velkovsky, Phys. Rev. Lett. **81** (1998) 53.
- [7] E. Dagotto, F. Karsch and A. Moreo, Phys. Lett. **169B** (1986) 421.
- [8] E. Dagotto, A. Moreo, U. Wolff, Phys. Lett. **186B** (1987) 395.
- [9] C. Baillie et.al., Phys. Lett. **197B** (1987) 195.
- [10] G.W. Carter and D. Diakonov, hep-ph/9812445 and references therein.
- [11] H. Kluberg-Stern, A. Morel and B. Petersson, Nucl. Phys. **B215** (1983) 527.
- [12] T. Schäfer, E.V. Shuryak and J.J.M. Verbaarschot, Nucl. Phys. **B412** (1994) 143.
- [13] M.-P. Lombardo, J.B. Kogut and D.K. Sinclair, Phys. Rev. **D54** (1996) 2303.
- [14] J.B. Kogut, M.-P. Lombardo and D.K. Sinclair, Phys. Rev. **D51** (1995) 1282.
- [15] M.E. Peskin, Nucl. Phys. **B175** (1980) 197.
- [16] S.J. Hands and M. Teper, Nucl. Phys. **B347** (1990) 819.
- [17] J.J. M. Verbaarschot, Phys. Rev. Lett. **72** (1994); M.A. Halasz and J.J.M. Verbaarschot, Phys. Rev. Lett. **74** (1995) 3920.
- [18] S. Hands, in preparation.
- [19] S.J. Hands and S.E. Morrison, hep-lat/9807033.
- [20] Th. Schaefer, Nucl. Phys. **A642** (1998) 45.
- [21] Private communication with M. Oevers and I. Barbour.
- [22] T. Banks and A. Zaks, Nucl. Phys. **B196** (1982) 189.
- [23] T. Appelquist and F. Sannino, hep-ph/9806409.
- [24] J.B. Kogut, J. Polonyi, H.W. Wyld, D.K. Sinclair, Phys. Rev. **D31** (1985) 3307.
- [25] A. Kocić, J.B. Kogut and M.-P. Lombardo, Nucl. Phys. **B398** (1993) 376.
- [26] E.V. Shuryak, Comments Nucl. Phys. **21**, (1994) 235.
- [27] M. Stephanov and A. Zhitnitsky, work in progress, communicated by M. Stephanov.
- [28] S.E. Morrison and S.J. Hands, contribution to the workshop *Strong and Electroweak Matter*, Copenhagen, 2nd - 5th December 1998, hep-lat/9902012.
- [29] M.-P. Lombardo, to be submitted.

FIGURES

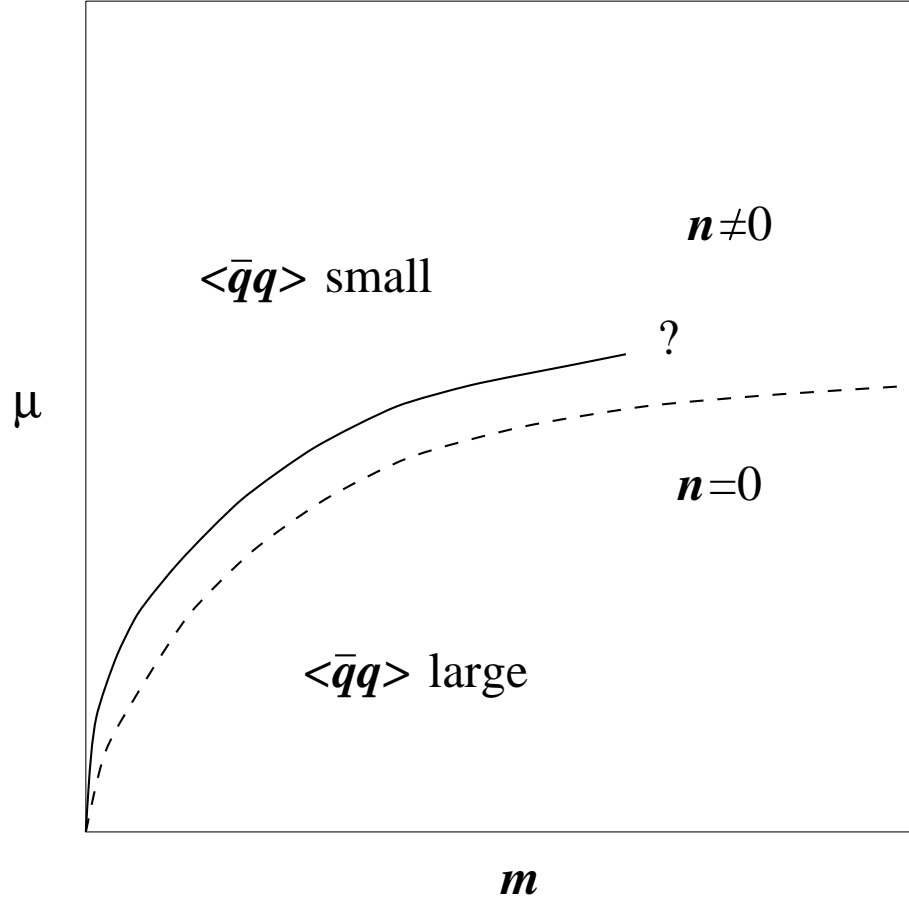


FIG. 1. Tentative phase diagram in the (m, μ) plane for the standard scenario

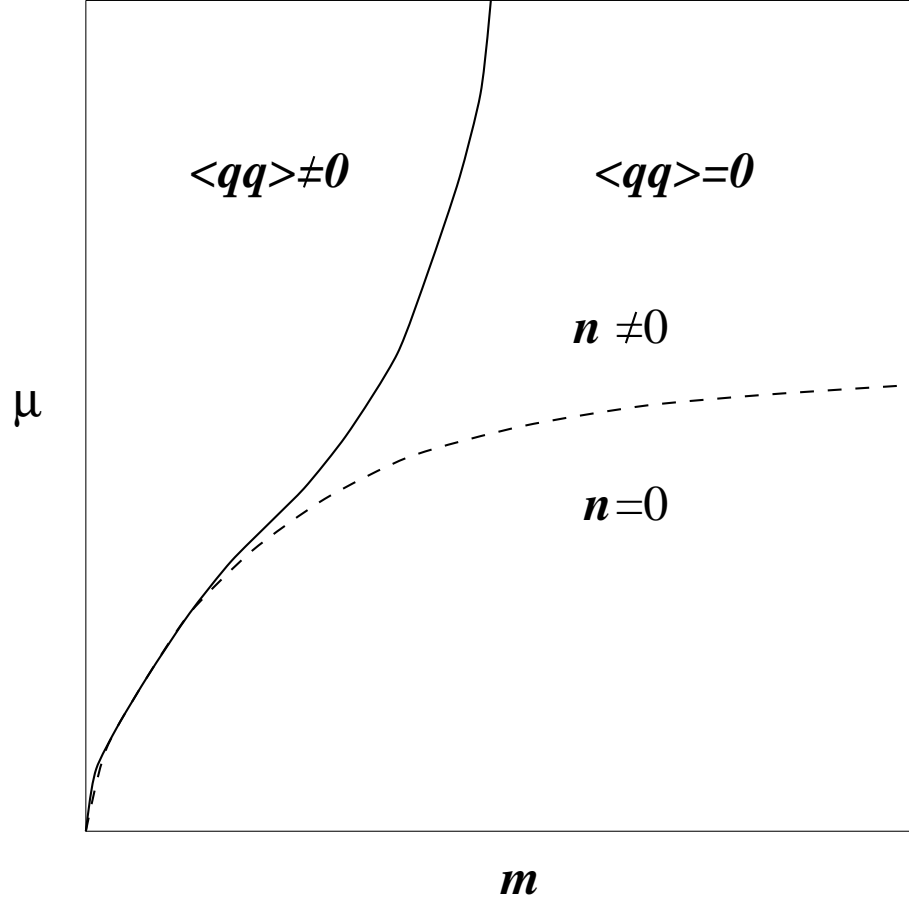


FIG. 2. Tentative phase diagram in the (m, μ) plane when a diquark condensate $\langle qq \rangle$ is considered

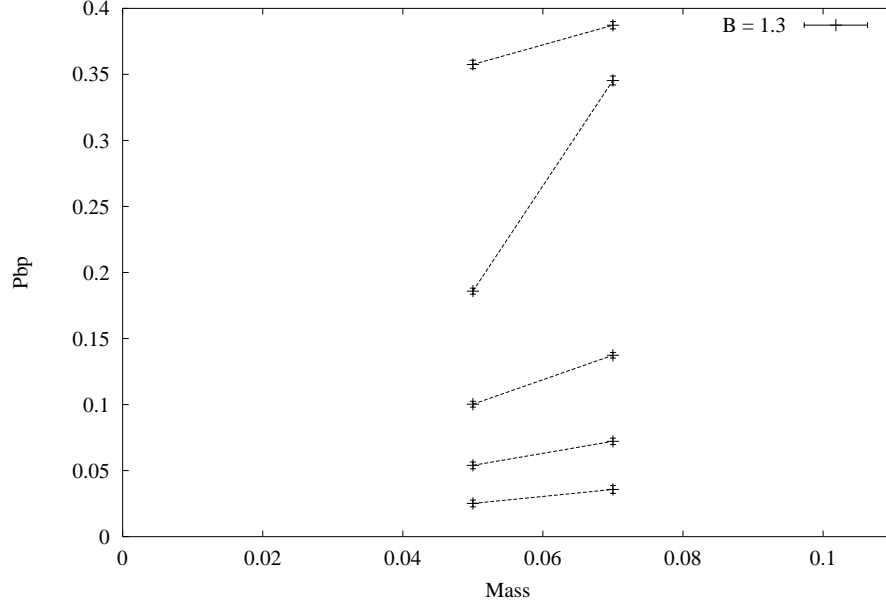


FIG. 3. $\langle \bar{q}q \rangle$ as a function of the bare mass for $\beta = 1.3$ (upper) at $\mu = 0, .2, .4, .6, .8$

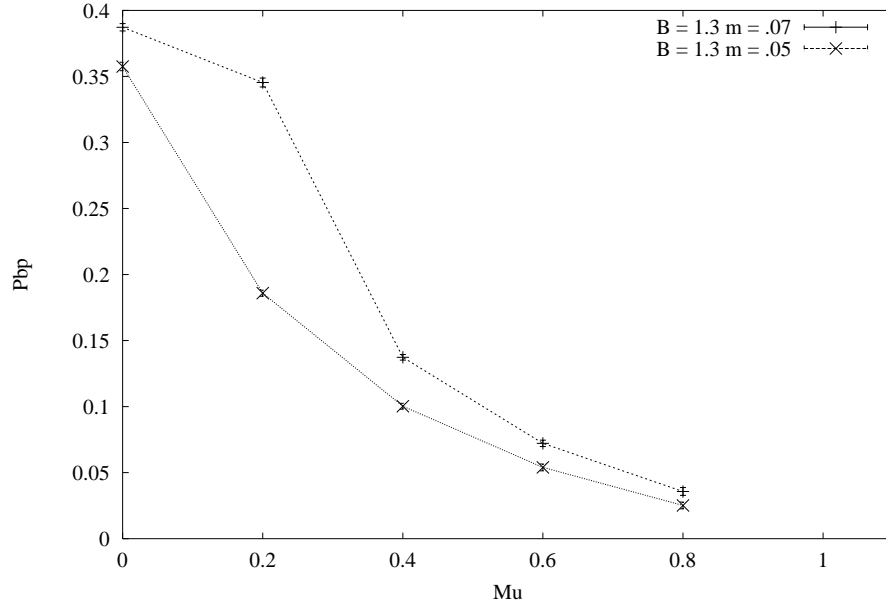


FIG. 4. $\langle \bar{q}q \rangle$ as a function of the chemical potential for $\beta = 1.3$ and masses as shown in the diagrams

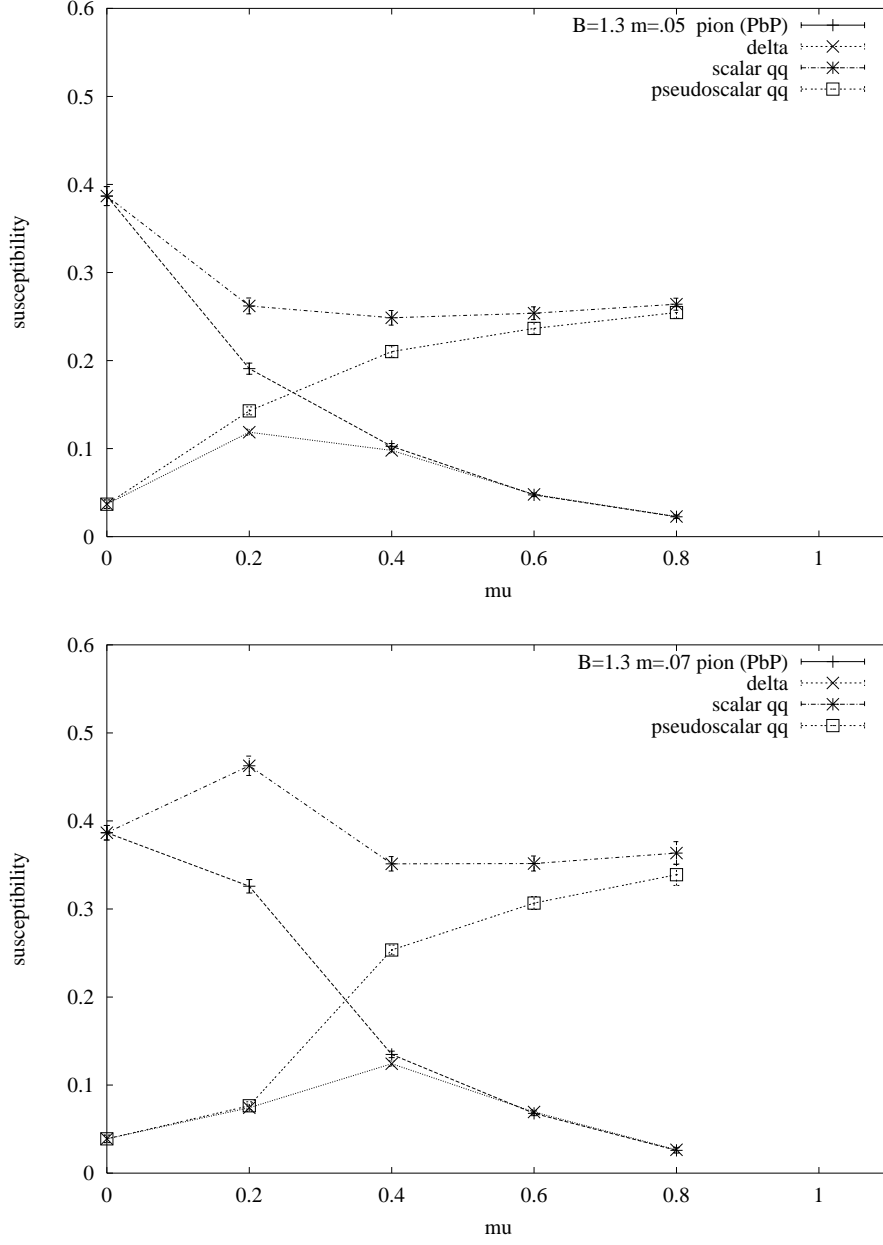


FIG. 5. Scalar and pseudoscalar susceptibilities for mesons and diquarks a function of μ at $\beta = 1.3$ and mass = .05 (upper) and mass = .07. See text for discussions

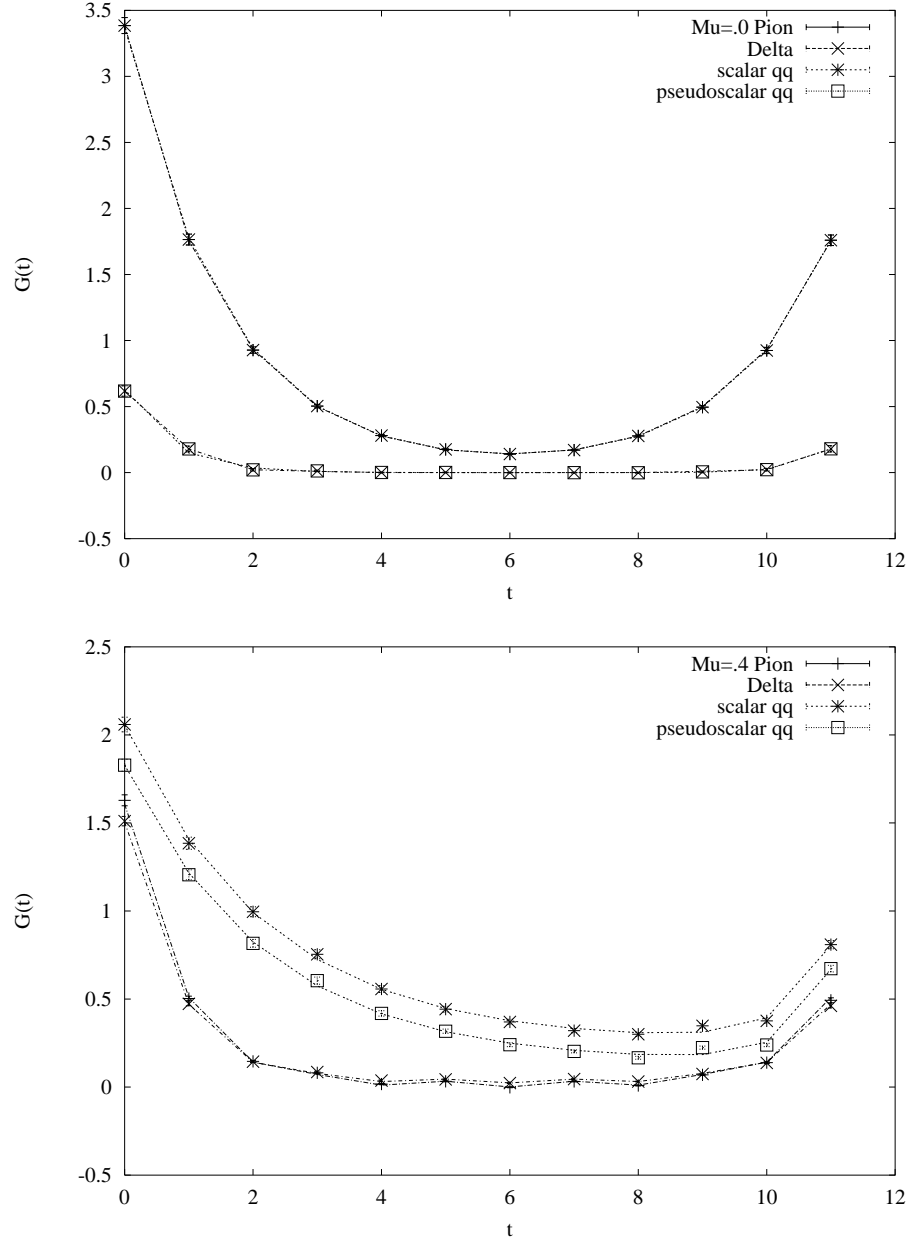


FIG. 6. Level ordering at $\mu = 0.0$ and $\mu = 0.4$

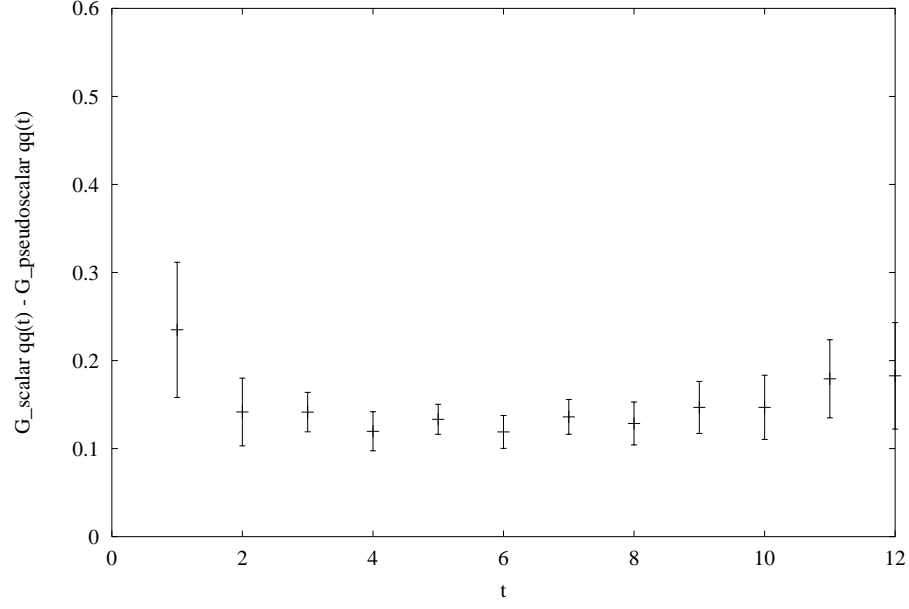


FIG. 7. Difference of the scalar and pseudoscalar diquark propagators as a function of the time distance, suggesting a) condensation in the scalar channel b) similar particle content in the two channels.

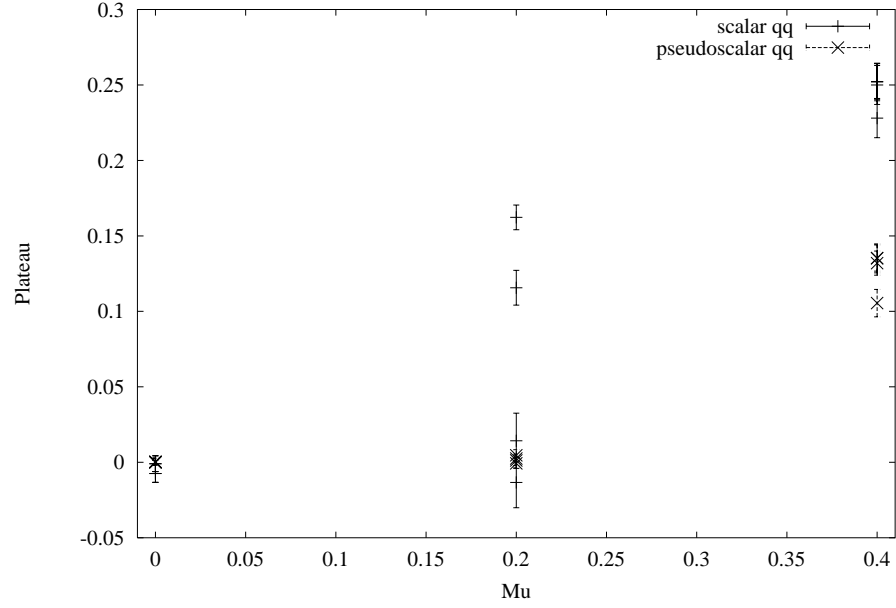


FIG. 8. Plateau p ($\simeq \langle \chi\chi \rangle^2$) from the fits of the scalar and pseudoscalar propagators

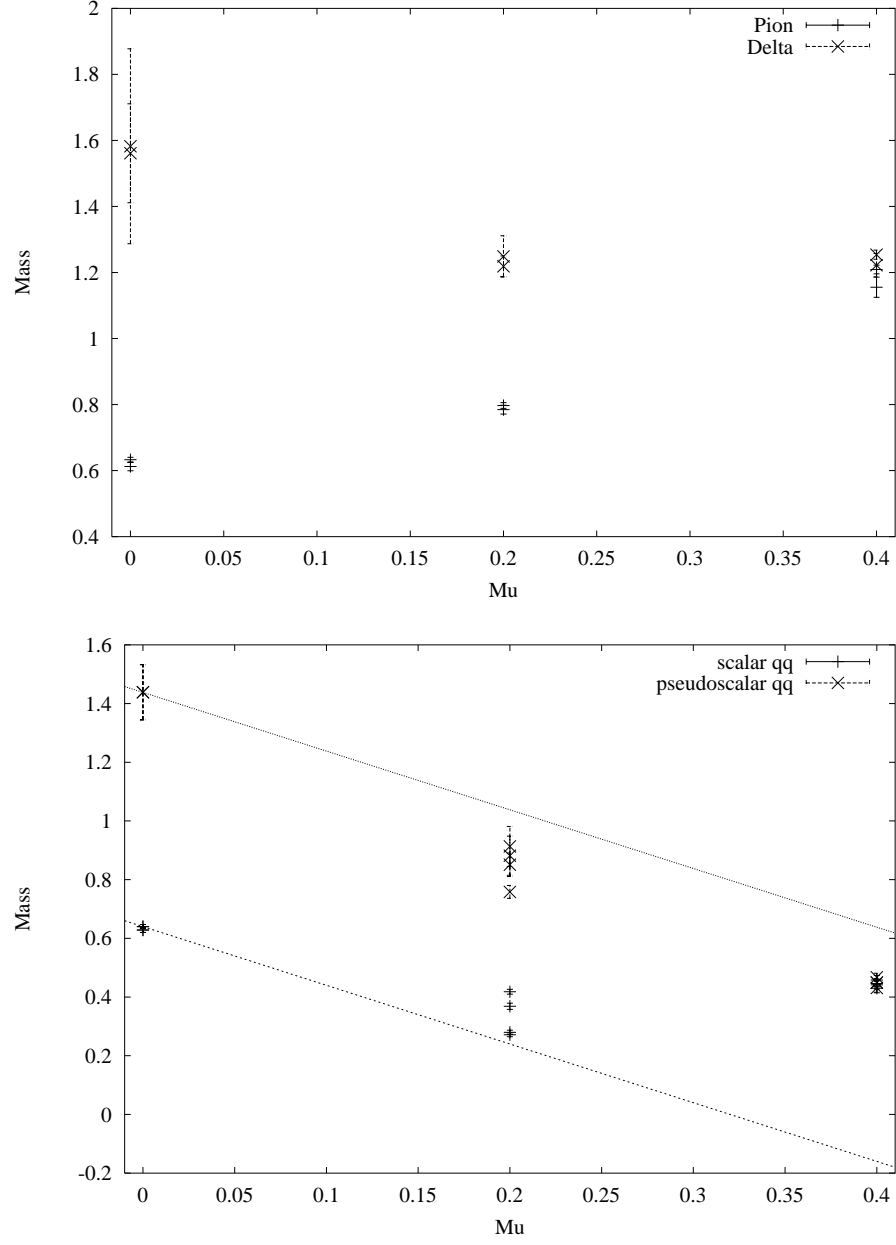


FIG. 9. Masses as a function of the chemical potential. For the diquarks we also show the naive prediction $m(\mu) = m(\mu = 0) - 2 * \mu$